Biases in the Modeled Surface Radiative Fluxes in Column Climate Simulations of SHEBA in May

J. O. Pinto, J. A. Curry, and A. H. Lynch
Program in Atmospheric and Oceanic Sciences
University of Colorado
Boulder, Colorado

Introduction

The single-column model (SCM) version of the Arctic Regional Climate System Model (ARCSyM) has recently been evaluated using data collected during SHEBA (Surface Heat Budget of the Arctic) (Pinto et al. 1999; Curry et al. 1999). Observations were obtained from surface-based and airborne measurements. Large biases are found in the modeled surface radiative fluxes. In this study, we will discuss the cause of biases in the modeled surface radiative fluxes in ARCSyM identified in May.

Observations

The SHEBA site consists of a Canadian ice breaker, the Des Groseilliers, which supports several instruments on-board and surrounding the ship. The ice breaker was moored to a multi-year ice floe in the Beaufort Sea. By the beginning of May the station had drifted northwestward to approximately 75.9 N, 165.8 W. Cloud properties were observed with a 35-GHz cloud radar, a Microwave Radiometer, and a Dual-Polarization Aerosol and Backscatter Unattended Lidar (DABUL) located on the deck of the ship. The cloud radar is used to determine cloud boundaries and cloud fraction while the lidar is used to discriminate particle phase and identify cloud base (Figure 1a). Liquid water path (LWP) and precipitable water (PW) can be estimated from the two brightness temperatures observed with the Microwave Radiometer. Several meteorological observing stations were set up on the surrounding ice floes. Radiometric measurements were obtained with Eppley pyranometers and pyrgeometers on a 2-m stand located near the 20-m flux tower.

Rawinsondes were launched every 6 hours during the aircraft intensive observation periods (IOPs). The rawinsondes used Vaisala components. These IOPs lasted from April 8 to July 30. The rawinsonde data have been gridded to the mean height of each level in the model (discussed below) using a nearest neighbor approach (Figure 1b). The air temperature is seen to warm with time at each height. The first week is characterized by the presence of an inversion layer between 1 km and 2 km. Temperatures in the lowest 1 km warm from -20 °C to 0 °C during the month, while the height of the tropopause is seen to increase from 8 km to 11 km during the month.

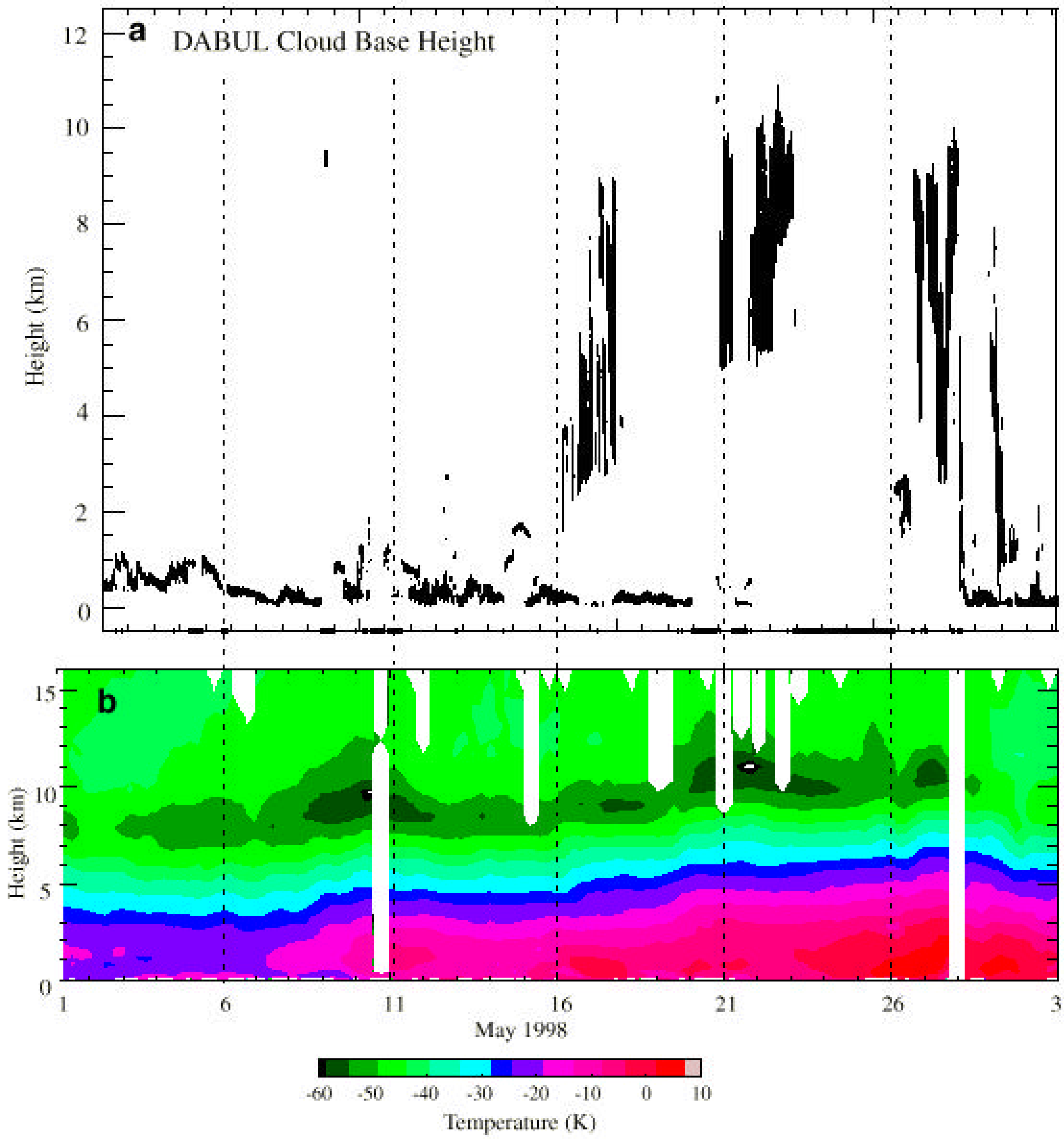

Figure 1. Time-height cross sections of (a) cloud base height from DABUL, and (b) air temperatures from rawinsonde. Missing data in (b) is blank.

The moisture field experiences a net moistening during the month that is interrupted by several dry periods. This is depicted in the time series of PW given in Figure 2a. It is seen that the atmosphere is extremely dry during two periods (May 1-10 and May 21-26). A period of strong moistening takes place on May 10 and during the last week of May. Comparing PW obtained from rawinsondes with that obtained with the Microwave Radiometer reveals the slight dry bias in the PW obtained from the rawinsonde data.

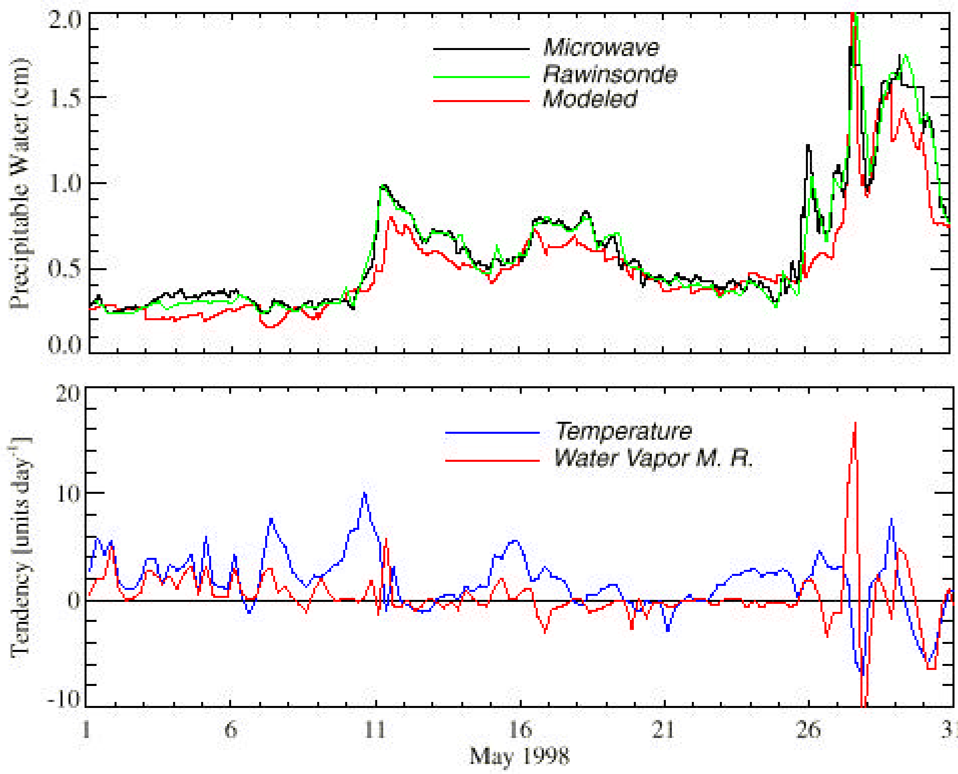

Figure 2. Time series of (a) modeled and observed PW and (b) vertically averaged large-scale advective tendencies. Vertical averaging done for the 800-mb to 1000-mb layer.

A column version of the ARCSyM has been developed for testing general circulation models (GCMs) parameterizations in the arctic (Pinto et al. 1999). The full three-dimensional (3-D) version of ARCSyM is described in detail by Lynch et al. (1995).

The cloud microphysics are modeled using the bulk parameterization developed by Dudhia (1989). This parameterization uses just two prognostic equations: one for cloud water and one for precipitation. Mixed-phase clouds cannot be produced. A threshold temperature is employed to determine whether ice-phase or liquid-phase microphysical processes are employed. A threshold temperature of 255.16 K is chosen based on observations obtained during the Beaufort and Arctic Storms Experiment (BASE) and SHEBA.

The radiative transfer is treated using separate two-stream parameterizations for shortwave and longwave radiation. The longwave fluxes are calculated using rapid radiative transfer model (RRTM) (Mlawer et al. 1997). The cloud radiative properties vary spectrally following the parameterizations of Hu and Stamnes (1993) for liquid and Ebert and Curry (1992) for ice. The effective radii for liquid and ice clouds are specified to be 7 μm and 40 μm, respectively. Shortwave radiative transfer is modeled using the two-stream scheme described by Briegleb (1992) with liquid clouds treated using Slingo (1989) and ice clouds after Ebert and Curry (1992).

The lower boundary conditions are specified in the model. The surface is assumed to be a mixture of multi-year sea ice and leads (open water). The open water fraction was set at 5%. The surface skin temperature is specified from the observations obtained at the 20-m tower. The albedo of the snow surface was specified at 0.76 from Regional Atmospheric Modeling System (RAMS) observations obtained during a low-level box pattern flown beneath a fairly homogenous cloud layer on May 18. The ocean surface temperature in leads is assumed to be -1.8 °C.

The model uses a sigma coordinate system (39 levels + the surface) with the highest resolution in the lowest 1.5 km.

The large-scale 3-D advective tendencies of temperature, moisture, and winds are supplied by the European Centre for Medium-Range Weather Forecasting (ECMWF) column data set. The large-scale, vertically averaged total advective tendencies for temperature and water vapor mixing ratio are shown in Figure 2b. The periods of positive large-scale moisture advection coincide with peaks in the observed PW. However, the strength of the moisture advection estimated by ECMWF may not have been large enough as evidenced by the underpredicted PW amounts in the ECMWF simulation (Figure 2a).

Results

The model is run for 30 consecutive days beginning 0000 UTC on May 1. Hourly advective forcing provided by ECMWF and surface temperatures from the 20-m tower are linearly interpolated between hours.

Errors in the downward radiative fluxes at the surface are substantial in the ARCSyM simulation. The biases in the modeled monthly mean downward fluxes given in Table 1 are consistent with an underpredicted cloud amount and/or cloud optical thickness. The ECMWF results show a similar but less drastic bias. The mean biases in the downward longwave and shortwave fluxes at the surface are 7% and 17%, respectively. Substantially larger errors are evident in the comparison of time series of radiative fluxes shown in Figure 3. The modeled downward longwave flux may be anywhere from ±30% of the observed value while the modeled shortwave flux can be off from the observed value by as much as ±50%.

The largest errors arise from a poor simulation of the cloud field. It is seen that the modeled cloud field (Figure 3) has the same general pattern as that observed (Figure 1b) with low cloud dominating the first two weeks of May and high cloud dominating weeks three and four. However, the modeled clouds below 2 km are typically shorter lived than observed. This makes up a large fraction of the discrepancy between the modeled and observed total cloud fraction reported in Table 1. Errors in the downward radiative fluxes caused by missing cloud events are evident in Figure 3 on May 9, 16, 18, and 21. The prediction of cloud when none is observed (e.g., May 1) is less common, but does lead to a positive bias in the downward longwave flux and a negative bias in the downward shortwave flux. Errors in the simulated cloud water paths also contribute to biases in the surface radiative fluxes reported in Table 1, particularly in the shortwave. An example of this is evident in the shortwave fluxes on May 13-16.

Table 1. Monthly means for May 1999.

	Units	Observed	ECMWF	ARCSyM
Cloud fraction		0.82	0.69	0.51
Cloud top	km	3.3	3.8	3.2
Cloud base	km	1.2	0.8	1.3
PW	cm	0.56-0.61	0.52	0.46
LWP	g m^{-2}	43	9	11
DSWR	W m^{-2}	248	275	291
DLWR	W m^{-2}	244	231	227

DLWR = downwelling longwave radiation.
DSWR = downwelling shortwave radiation.
LWP = liquid water path.

The modeled monthly mean LWP is severely underpredicted. This is due to a severe underprediction of the number of cloud events by the model and an underprediction of the cloud water path when cloud occurrence is accurately predicted. This is evident in Figure 4, which indicates that the cloud water path is underpredicted when the observed water path exceeds 65 g m^{-2}. There is a great deal of scatter as well (r.m.s.e = 70 g m^{-2}) indicating that the model has little skill at predicting cloud water path.

Errors in the modeled temperature and moisture profiles affect the modeled radiative fluxes at the surface by influencing the evolution of clouds and, in the longwave, by determining the effective emission temperature of the atmosphere. The latter is evident in the longwave fluxes during the first 10 days of the simulation. During this time the low clouds tend to occur within a layer that is modeled to be much warmer than observed. This results in a positive bias in the downward longwave flux at the surface (e.g., May 2-4). The modeled monthly mean temperature below 1.5 km is as much as 4 K too warm (Figure 5). Since most of the clouds are modeled to occur below 2 km, the emission temperature bias will result in a positive bias in the downward longwave flux at the surface. Since the modeled mean downward longwave flux in ARCSyM is too small, this bias is apparently overwhelmed by the cloud fraction bias.

Cloud fraction is underpredicted in the model due to the modeled profile being too dry. The temperature and moisture biases combine to two regions with dry biases: above 7.5 km and below 2 km. Below 2 km these biases result in a reduction in the relative humidity with respect to water of as much as 10%. This is an extremely important finding because it shows how cloud fraction in GCMs is extremely sensitive to small changes in relative humidity.

A comparison between modeled and observed downward radiative fluxes at the surface under clear-sky conditions was made. The modeled clear-sky longwave fluxes have a negative bias of about -6 W m^{-2}. Off-line calculations indicate that RRTM has a bias of about -3 W m^{-2}. This indicates that errors in the modeled temperature and moisture profiles contribute about half of the total bias. Comparison between modeled and observed clear-sky shortwave fluxes reveals a large positive bias in the modeled fluxes

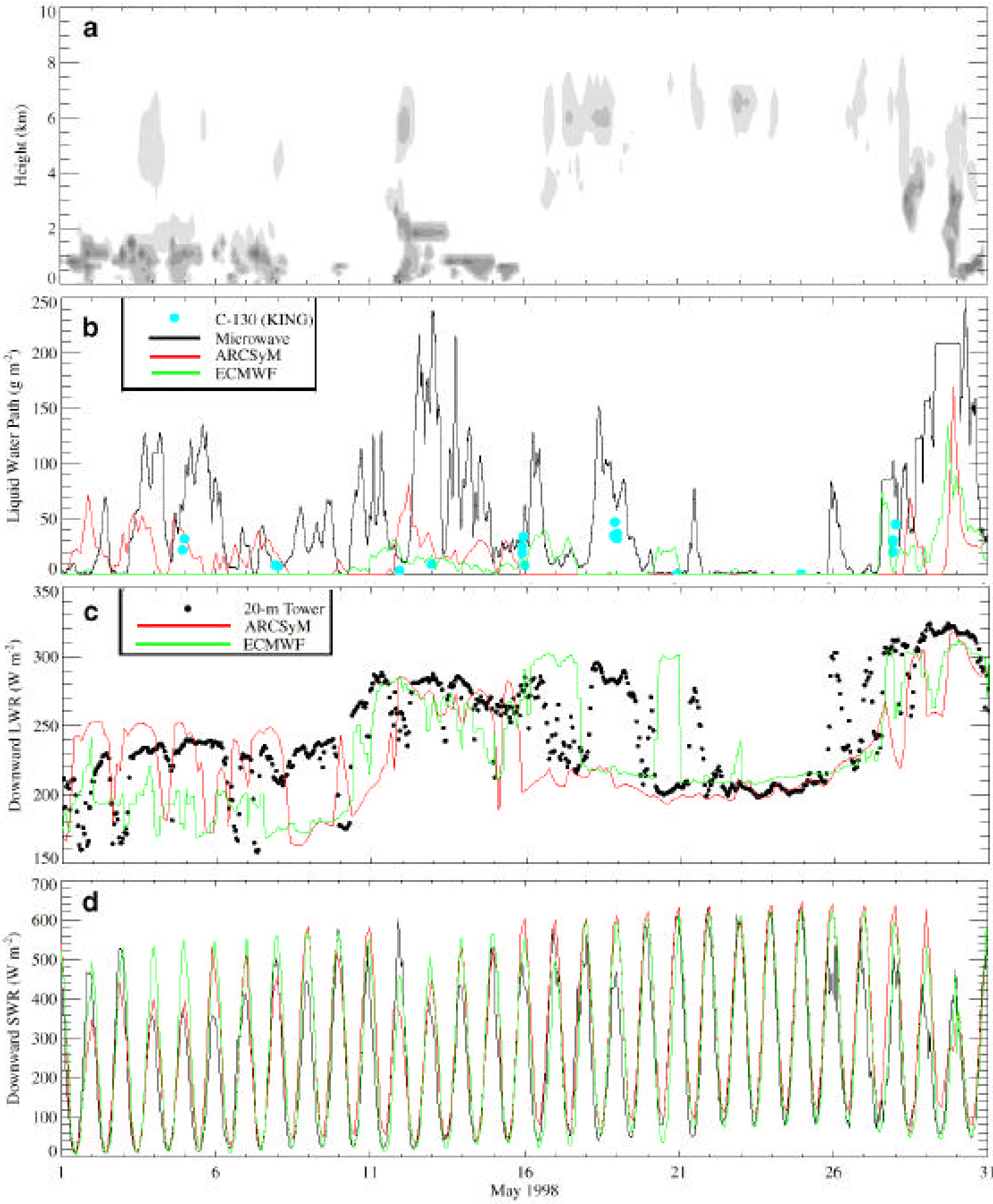

Figure 3. Results from ARCSyM simulation and ECMWF SHEBA column data set including (a) cloud water mixing ratio, (b) LWP, (c) downward longwave radiative flux at the surface, and (d) downward shortwave radiative flux at the surface. ARCSyM data are 3 hourly and ECMWF data are hourly. LWPs from the Microwave Radiometer have been smoothed with a 2-hour running average. Observed surface radiative fluxes (black) are hourly mean values. LWPs were also obtained from aircraft by vertically integrating King Probe measurements of liquid water content made during vertical profiles through the cloud layers.

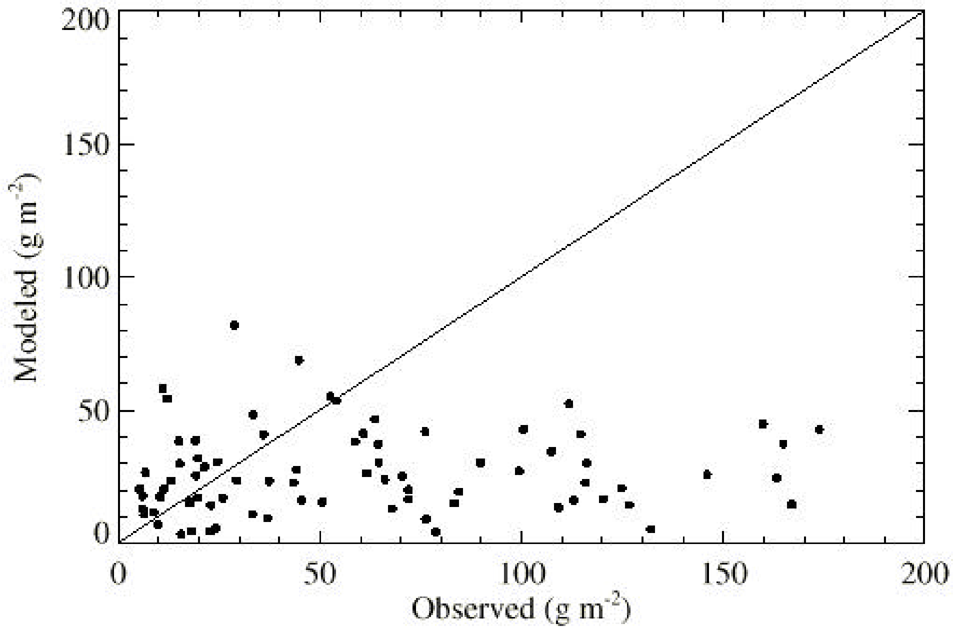

Figure 4. Modeled LWP versus observed LWP obtained from the Microwave Radiometer.

(Figure 6). This bias is evident at all zenith angels; however, its relative size is greatest at the larger zenith angles. This bias may be related to the lack of treating aerosol radiative properties by the shortwave scheme.

Comparing the modeled and observed relationship between LWP and downward shortwave flux at the surface reveals an additional source of error for the modeled surface radiative fluxes. The downward shortwave flux is underestimated when the LWP exceeds 50 g m^{-2} (Figure 7). This may be due to inadequate treatment of multiple reflections between the surface and cloud or underestimated shortwave attenuation in the model.

Conclusions

The results of this study indicate the importance of properly specifying the large-scale forcing in the model. During the month of May, the ECMWF forcing appears to have a warm and dry bias in the lowest 2 km. This may be related to the inadequate treatment of the surface temperature prediction in ECMWF. Re-analyses performed with a better treatment of the surface will likely alleviate some of the biases reported in this study. Biases will still exist that are a function of the parameterization package used by the large-scale model. By combining the available large-scale forcing with other forcing techniques such as observational nudging, a better representation of the temperature and moisture fields may be realized.

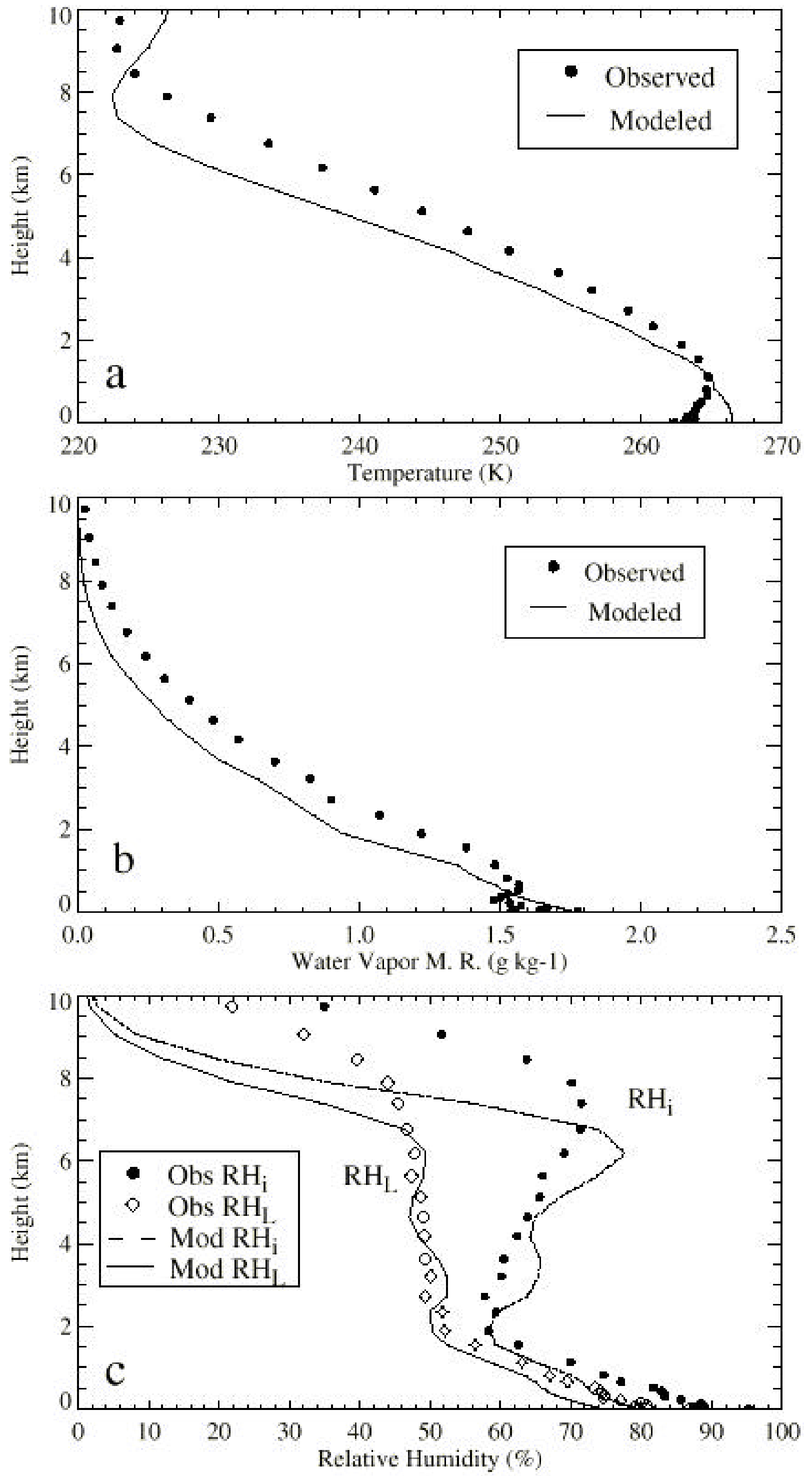

Figure 5. Monthly mean profiles of (a) temperature, (b) water vapor mixing ratio, and (c) relative humidity with respect to water and ice observed (symbols) and modeled (lines) for the month of May. Observations are from rawinsonde data. Model results are from 30-day ARCSyM simulation.

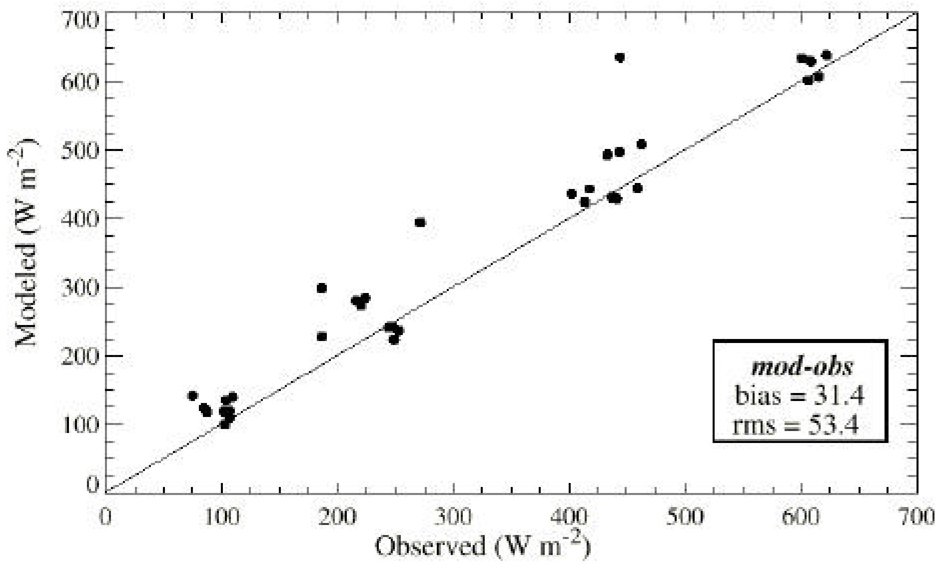

Figure 6. Modeled versus observed downward shortwave flux at the surface under clear-sky conditions.

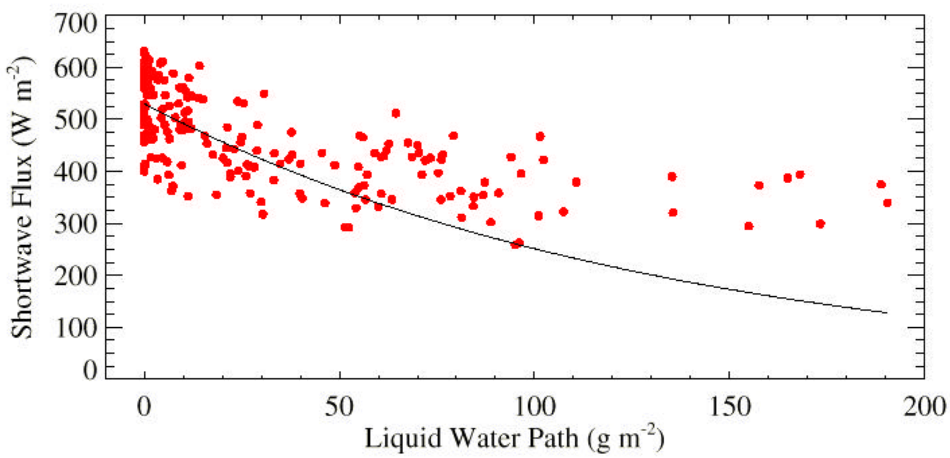

Figure 7. Observed relationship between downward shortwave flux at the surface and LWP (red dots) compared with relationship obtained with model (line) for zenith angles greater than 60°. Line obtained using a least squares fit to the model data, using the non-linear function SWR = A1*exp((A2-LWP)/A3)), where A1, A2, and A3 are the coefficients determined by the least squares fit.

Despite the forcing errors, we were able to elucidate several sources of error in the modeled radiative fluxes at the surface in ARCSyM. The importance of treating aerosols for clear-sky shortwave computations was described. The cloudy-sky shortwave calculations indicated that at large optical depths the model underpredicted the downward flux at the surface. This may be caused by an inadequate treatment of surface albedo or errors in the shortwave attenuation by clouds. The RRTM scheme has a clear-sky bias in the longwave of about 1-2 W m^{-2}. This is small compared with the 6 W m^{-2} bias resulting from errors in the modeled thermodynamic structure of the atmosphere.

Continued analysis of BASE, FIRE-ACE (First ISCCP [International Satellite Cloud Climatology Program] Regional Experiment-Aerosol Characterization Experiment), and SHEBA data will be used to further characterize problems with model parameterizations and to improve the treatment of clouds and radiation in the arctic.

Acknowledgments

We are greatly indebted to those who collected and provided the SHEBA data including C. Bretherton, C. Fairall, O. Persson, and J. Intrieri.

References

Briegleb, B. P., 1992: Delta-Eddington approximation for solar radiation in the NCAR Community Climate Model. *J. Geophys. Res*., **97**, 7603-7612.

Curry, J. A., et al., 1999: FIRE Arctic clouds experiment. *Bull. Amer. Meteor. Soc*. Accepted.

Dudhia, J., 1989: Numerical study of convection observed during the winter monsoon experiment using a mesoscale two-dimensional model. *J. Atmos. Sci*., **46**, 3077-3107.

Ebert, E. E., and J. A. Curry, 1992: A parameterization of ice cloud optical properties for climate models. *J. Geophys. Res*., **72**, 3831-3836.

Hu, X. Y., and K. Stamnes, 1993: An accurate parameterization of the radiative properties of water clouds suitable for use in climate models. *J. Climate*, **6**, 728-742.

Lynch, A. H., W. L. Chapman, J. E. Walsh, and G. Weller, 1995: Development of a regional climate model of the western Arctic. *J. Climate*, **8**, 1555-1570.

Mlawer, E. J., S. J. Taubman, P. D. Brown, M. J. Iacono, and S. A. Clough, 1997: Radiative transfer for inhomogeneous atmospheres: RRTM, a validated correlated-k model for the long-wave. *J. Geophys. Res*., **102**, 16663-16682.

Pinto, J. O., J. A. Curry, A. H. Lynch, and O. Persson, 1999: Modeling clouds and radiation for the November 1997 period of SHEBA using a column climate model. *J. Geophys. Res*., **104**, 6661-6678.

Slingo, A., 1989: A GCM parameterization for shortwave radiative properties of water clouds. *J. Atmos. Sci*., **46**, 1419-1427.